



ELSEVIER

Journal of Nuclear Materials 294 (2001) 232–240

**Journal of
nuclear
materials**

www.elsevier.nl/locate/jnucmat

Thermodynamic properties of lanthanide metals in liquid bismuth

Hajimu Yamana ^{a,*}, Jiawei Sheng ^a, Naohiko Souda ^b, Hirotake Moriyama ^a^a *Research Reactor Institute, Kyoto University, Noda, Kumatori-cho, Sennan-gun, Osaka-fu 590-0494, Japan*^b *Graduate School of Engineering, Kyoto University, Yoshida, Sakyo-ku, Kyoto-shi 606-8501, Japan*

Received 27 July 2000; accepted 28 January 2001

Abstract

Thermodynamic quantities of La, Gd, Tb, and Dy in liquid bismuth were experimentally determined by electromotive force (EMF) measurement using a cell consisting of molten alkaline chloride and liquid bismuth. Excess Gibbs energy changes and activity coefficients were determined at varying concentrations and temperatures. Through their temperature dependence, corresponding enthalpy changes and entropy changes were determined. The excess enthalpy changes of La, Gd, Tb, and Dy in liquid bismuth in a temperature range from 850 to 1100 K were evaluated to be, -221.54 ± 2.31 , -202.25 ± 1.80 , -199.83 ± 0.55 , and -193.80 ± 0.99 kJ/mol, respectively. The systematic variation of excess enthalpy change of lanthanides along the 4f-series was discussed. As a result, it was found that the excess enthalpy changes of La, Gd, Tb, Dy, and Er are likely to depend linearly on the 2/3 power of their metallic volume. © 2001 Elsevier Science B.V. All rights reserved.

PACS: 82.60.Lf; 82.60

1. Introduction

The pyrometallurgical liquid–liquid extraction of lanthanides and actinides (f-elements, hereafter) between molten chloride and liquid metal is one of the alternative techniques for the future group separation of actinides and lanthanides [1,2]. In this extraction system, in which molten chloride salt and liquid metal are used, the solute cations in the molten salt phase are reduced by metallic Li, and extracted into the liquid metal phase by forming a liquid alloy. The extraction and separation performance of lanthanides and actinides by this pyrometallurgical extraction system mainly depends on the standard Gibbs energy of formation of their chlorides, but it should be remembered that it is significantly influenced by their activity coefficients in both phases [3].

In the liquid metal phase, the solute metals are considered to be thermodynamically stabilized by forming chemical complexes with the solvent metals. This additional stabilization of f-element metals by the interaction with the solvent metals, such as zinc and bismuth, results in deeply negative excess partial molar Gibbs energies of f-elements in these liquid metals. This is responsible for the low activity coefficients of f-elements in these metals, by which the extraction of f-elements to the metal phase is promoted.

In the previous paper [3], we studied the extraction behaviors of trivalent f-elements in a liquid–liquid extraction system of molten alkaline chloride and liquid bismuth, and their thermodynamic properties were systematized. In that study, for estimating the standard Gibbs energy changes of formation of the liquid alloy of various lanthanides with bismuth, we applied a simplified linear relation of them with the 2/3 power of the metallic volumes of lanthanides. This linear relation was determined by the least-squares fitting of the reported values for some trivalent lanthanides [4–6]. However, since the number of reported lanthanides

* Corresponding author. Tel.: +81-724 51 2442; fax: +81-724 51 2634.

E-mail address: yamana@hl.rri.kyoto-u.ac.jp (H. Yamana).

is limited, this linear relation still has a large uncertainty.

Thus, the purpose of this study is to determine experimentally some unreported excess partial molar thermodynamic quantities of lanthanides in liquid bismuth, and to systematize them in view of the characteristic pyrochemistry of f-elements. By enhancing our understanding on the systematic trend of the excess thermodynamic properties of f-elements in liquid bismuth, we will be able to predict the separation behavior of f-elements in similar pyrometallurgical extraction systems using bismuth as a metal solvent. For this purpose, four lanthanides (La, Gd, Tb, and Dy) were tested to determine their excess thermodynamic quantities in bismuth by electromotive force (EMF) measurement technique. Tb, and Dy were chosen because they were expected to fill the vacancy of the linked data of lanthanide series. La and Gd were chosen to verify the reliability of our measurement technique by comparing them with the already reported values [4–6].

2. Thermodynamic basis of the EMF measurement

In this study, the solute metal and solvent metal are denoted by M and B, respectively. In the following thermodynamic expressions, M(in B) means solute metal M dissolved in liquid metal B, M(solid) and M(liquid) mean the solid and liquid states of pure metal M, respectively. In this paper, M represents trivalent lanthanide metal and B represents bismuth as a solvent metal.

In the mixture of two liquid metals, the chemical potential of solute metal M in solvent metal B, denoted by $\mu_{M(\text{in B})}$, is given by

$$\mu_{M(\text{in B})} = \mu_{M(\text{liquid})} + RT \ln x_{M(\text{in B})} + \mu_{M(\text{in B})}^{\text{ex}}, \quad (1)$$

where $\mu_{M(\text{liquid})}$ is the chemical potential of pure liquid M, $x_{M(\text{in B})}$ is the mole fraction of M in B, and $\mu_{M(\text{in B})}^{\text{ex}}$ is the excess chemical potential of M in B. When $\mu_{M(\text{in B})}$ is discussed in reference to the chemical potential of solid M, Eq. (2):

$$\mu_{M(\text{in B})} - \mu_{M(\text{solid})} = \Delta\mu_{M}^{\text{fusion}} + RT \ln x_{M(\text{in B})} + \mu_{M(\text{in B})}^{\text{ex}} \quad (2)$$

is more convenient, and it directly indicates the thermodynamic relation of this study. In Eq. (2), $\Delta\mu_{M}^{\text{fusion}}$, which is defined by Eq. (3), denotes the chemical potential difference between solid M and hypothetical super-cooled state of liquid M at experimental temperatures lower than melting point.

$$\Delta\mu_{M}^{\text{fusion}} = \mu_{M(\text{liquid})} - \mu_{M(\text{solid})}. \quad (3)$$

$\mu_{M(\text{solid})}$ is calculated by the published thermodynamical functions with specific coefficients for relevant solid phases of M [7]. Hypothetical $\mu_{M(\text{liquid})}$ is calculated by

extrapolating the function for the liquid phase to the temperatures lower than melting point. Thus, $\mu_{M(\text{in B})}^{\text{ex}}$ in Eq. (2) is recognized as the excess function associated with mixing hypothetical super-cooled liquid of M with liquid metal B. The difference of the chemical potentials between M(in B) and M(solid) generates EMF (ΔE) when the following cell is configured:

M(solid)|molten salt|M(in B).

Since the difference of the chemical potentials equals $-nF\Delta E$, Eq. (4):

$$\Delta E = -\frac{1}{nF} \Delta\mu_{M}^{\text{fusion}} - \frac{RT}{nF} \ln x_{M(\text{in B})} - \frac{1}{nF} \mu_{M(\text{in B})}^{\text{ex}} \quad (4)$$

can be obtained as a function of $\Delta\mu_{M}^{\text{fusion}}$, $\ln x_{M(\text{in B})}$, and $\mu_{M(\text{in B})}^{\text{ex}}$. By adapting experimentally observed ΔE and $\ln x_{M(\text{in B})}$, $\mu_{M(\text{in B})}^{\text{ex}}$ can be calculated by Eq. (5):

$$\mu_{M(\text{in B})}^{\text{ex}} = -nF\Delta E - \Delta\mu_{M}^{\text{fusion}} - RT \ln x_{M(\text{in B})}. \quad (5)$$

The activity coefficient $\ln f_{M(\text{in B})}$ can be calculated by Eq. (6):

$$\mu_{M(\text{in B})}^{\text{ex}} = RT \ln f_{M(\text{in B})}. \quad (6)$$

Since a chemical potential of solute metal M is regarded as a standard Gibbs energy change per mole of M, $\mu_{M(\text{in B})}^{\text{ex}}$ and $\Delta\mu_{M}^{\text{fusion}}$ in Eqs. (5) and (6) can be replaced by $\Delta G^{\text{ex}}[\text{M in B}]$ and $\Delta G^{\circ}_{\text{f}}[\text{M, liq}]$, respectively, which are the excess Gibbs energy change of M(in B) and standard Gibbs energy change of fusion of M, respectively. $\Delta G^{\circ}_{\text{f}}[\text{M in B}]$ which is the standard Gibbs energy change of formation of M(in B) is given by the sum of $\Delta G^{\text{ex}}[\text{M in B}]$ and $\Delta G^{\circ}_{\text{f}}[\text{M, liq}]$.

3. Experimental

EMF measurement method was applied to the following electrochemical cell

M(solid)|MCl₃ in LiCl–KCl|M(in B).

The experiments were performed in a vacuum-tight glove box filled with continuously purified Ar whose oxygen and humidity content was kept <1 ppm. The experimental system for the EMF measurement consists of finely sintered alumina crucible as a container of two liquids, liquid metal electrode lead by shielded Ta wire, pure lanthanide electrode, and thermocouple for temperature control. Ta wire was welded at one end of a rod ($3 \times 3 \times 25 \text{ mm}^3$) of 99.9% pure lanthanide metals, and this was used as a pure lanthanide electrode.

Before starting the experiment, the crucible was heated up to 773 K for several hours under vacuum in order to remove the humidity. About 36 g of eutectic mixture of LiCl and KCl (mole ratio of lithium to potassium = 59/41) and 133 g of pure bismuth were put in

the crucible with about 1 g of lanthanide metal, and then the temperature was raised up to desired values. After the desired temperature was achieved, the pure lanthanide electrode was immersed into the molten salt phase, and the EMF between the pure lanthanide electrode and liquid alloy electrode was measured by an electrometer. After immersing the pure lanthanide electrode, the variation of EMF was monitored for longer than 10 min, waiting for the stabilization of EMF. In many cases, the fluctuation of EMF settled into ± 1 mV within 10 min after starting the measurements, and in such cases it was recognized that the electrochemical equilibrium was achieved. The temperature was controlled to be within the range of $\pm 1^\circ\text{C}$.

Measurements for La, Gd, Tb, and Dy were performed at three or four different temperatures in a range from 730 to 1100 K. At each temperature, the concentration of lanthanide in bismuth phase was changed several times to record the EMF at different concentrations. For increasing the lanthanide concentration, small pieces of lanthanide metals were added. For decreasing the concentration, lanthanides were electrodeposited onto another cathode by using the liquid metal electrode as an anode. After the addition of lanthanide metals, the system was allowed to stand for over 5 h to ensure their perfect dissolution and an achievement of the concentration equilibrium in the two phases. After the removal of lanthanide by electrodeposition, it was allowed to stand for about 2 h to wait for the achievement of equilibrium. The sufficiency of these standing times was verified by following the variation of EMF over these periods. At every concentration, after EMF was recorded, a small portion of the metallic phase was taken as a sample. The samples were dissolved with diluted nitric acid, and the concentration of lanthanide in bismuth was analyzed by ICP-AES (ICPS-1000III, Shimadzu).

The eutectic mixture of LiCl-KCl was of 99.9% purity purchased from Anderson Physics Laboratory Engineered Materials, and it was used without further treatment. All other reagents used were of analytical grade purchased from Wako Pure Chemicals. The electrometer used was HG-5100 of Hokutodenko.

4. Experimental results and discussion

4.1. EMF measurements and activity coefficients

For all the elements and temperatures tested, observed EMF (denominated as ΔE) showed a roughly linear dependence on $\log x_{M(\text{in B})}$, suggesting that the variation of ΔE approximately obeys Eq. (4). An example of the observed dependence of ΔE on $\log x_{M(\text{in B})}$ is shown in Fig. 1 for the case of Gd. The lines drawn in Fig. 1 are those of theoretical slopes ($RT/3F$) which were

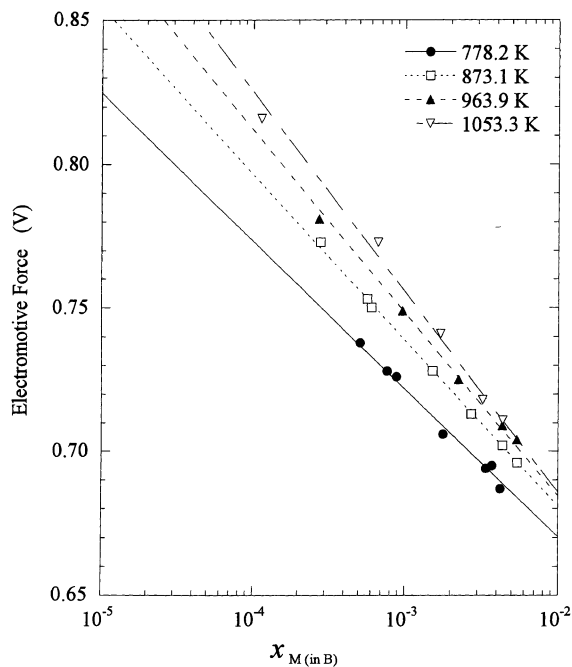


Fig. 1. Concentration dependence of the EMF determined for Gd.

obtained by applying the least-squares fitting method to the experimental data of every temperature. In spite of their rough linearities, there were cases where observed points showed slight deviations from the theoretical slopes. This suggests that the third term of Eq. (4) is not thoroughly constant over the tested concentration range, and that $\mu_{M(\text{in B})}^{\text{ex}}$ may depend on the concentration. Since this tendency is more explicitly understood in terms of $\ln f_{M(\text{in B})}$, $\log f_{M(\text{in B})}$ were calculated by Eqs. (5) and (6) by using all the pairs of ΔE and $\log x_{M(\text{in B})}$. Obtained $\log f_{M(\text{in B})}$'s are shown in Figs. 2(a)–(d) as functions of $\log x_{M(\text{in B})}$. The errors of $\log f_{M(\text{in B})}$ shown in the figures involve all the errors associated with the measurements. Major components of the errors are those accompanied by: (a) chemical analysis, from 10% for $x_{M(\text{in B})} = 10^{-6}$ to 2% for $x_{M(\text{in B})} = 10^{-2}$; (b) temperature measurement, constantly ± 1 K; and (c) EMF measurement, constantly ± 2 mV.

In Figs. 2(a)–(d), a slight dependence of $\log f_{M(\text{in B})}$ on $\log x_{M(\text{in B})}$ is clearly seen. The magnitude of the dependence is different for each different element. It can presumably be attributed to such a phenomenon as a weak interaction among the solute clusters, but it cannot be identified in this paper without a further accurate determination and a detailed theoretical consideration. In the past reports [4–6], $\log f_{M(\text{in B})}$ s were regarded as constant, and thus they were averaged over the tested concentration range, which should be validated only for the limited concentration range. On the other hand, for

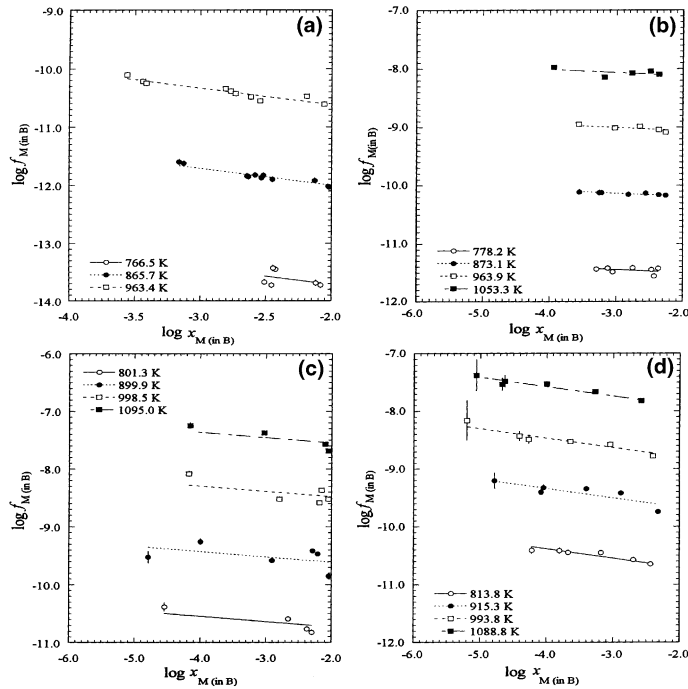


Fig. 2. Concentration dependence of the activity coefficients of: (a) La, (b) Gd, (c) Tb, and (d) Dy, in liquid bismuth.

knowing $\log f_{M(\text{in B})}$ at any desired concentration for a practical purpose, it is convenient to formulate them as simple functions of $\log x_{M(\text{in B})}$. In this study, they were formulated as linear functions by the least-squares fitting method, and they were expressed in the form of

$$\log f_{M(\text{in B})} = a \log x_{M(\text{in B})} + b. \quad (7)$$

The obtained coefficients for Eq. (7) are listed in Table 1. The uncertainties listed in Table 1 are the standard deviations of the data points around the fitted lines. In the past, $\log f_{M(\text{in B})}$ of La and Gd were determined by the same technique, and these data have been comprehensively summarized by Lebedev et al. [4]. In these past studies, it should be noted that the main body of the measurements was performed in the mole fraction range from ca. 10^{-3} to 5×10^{-2} , and in the temperature range from 753 to 953 K. Thus, in order to compare the present data with the reported ones, mole fraction $x_{M(\text{in B})} = 5 \times 10^{-3}$ was chosen as the representative concentration. Table 1 summarizes $\log f_{M(\text{in B})}$ at $x_{M(\text{in B})} = 5 \times 10^{-3}$ which were calculated by the coefficients of Table 1. In Table 1, the values of $\log f_{M(\text{in B})}$ for La and Gd determined in this study agree well with the reported values of the literatures within the range of uncertainties. Thereby, it was concluded that $\log f_{M(\text{in B})}$ for $x_{M(\text{in B})} = 5 \times 10^{-3}$ determined by the present study can be discussed together with the literature values.

4.2. Temperature dependence of $\log f_{M(\text{in B})}$ and thermodynamic quantities derived

In Fig. 3, calculated $\Delta G^{\text{ex}}[M \text{ in B}]$ for $x = 5 \times 10^{-3}$ are plotted versus Temperature (T/K). It should be noted that $\Delta G^{\text{ex}}[M \text{ in B}]$ do not show a thorough linearity on T over the temperature range from about 800–1100 K. If the excess enthalpy change $\Delta H^{\text{ex}}[M \text{ in B}]$ and corresponding excess entropy change $\Delta S^{\text{ex}}[M \text{ in B}]$ are kept constant over the tested temperature range, $\Delta G^{\text{ex}}[M \text{ in B}]$ should show a linear relation on T , giving $\Delta S^{\text{ex}}[M \text{ in B}]$ as its slope and $\Delta H^{\text{ex}}[M \text{ in B}]$ as its intercept. Therefore, the results shown in Fig. 3 suggest a possibility of varying $\Delta H^{\text{ex}}[M \text{ in B}]$ and/or $\Delta S^{\text{ex}}[M \text{ in B}]$ in this temperature range. On the other hand, it appears that three data points sided to higher temperatures show approximately a linearity, but the data point of the lowest temperature is likely to deviate from the line to the higher direction. Accordingly, it can be naturally considered that both $\Delta H^{\text{ex}}[M \text{ in B}]$ and $\Delta S^{\text{ex}}[M \text{ in B}]$ are kept constant only in the range sided to a higher temperature, but they possibly change at the temperature lower than about 850 K. It can presumably be attributed to the changing chemical properties of $M(\text{in B})$ in a lower temperature region, due to a change of the composition or structure of the clusters of M in liquid bismuth.

Since three data points of higher temperatures show quite a successful linearity, it can be considered that the

Table 1
Dependence of activity coefficient on the concentration

	Temperature (K)	$\log f_{M(\text{in B})} = a \log x_{M(\text{in B})} + b$			Lebedev et al. [4]	This study at $x_{M(\text{in B})} = 5 \times 10^{-3}$ ^a
		<i>a</i>	<i>b</i>	error		
La	766.5	-0.291	-14.30	0.11	-13.51	-13.63 ± 0.11
	865.7	-0.291	-12.59	0.04	-11.88	-11.92 ± 0.04
	963.4	-0.291	-11.20	0.05	-10.59	-10.53 ± 0.05
Gd	778.2	-0.054	-11.60	0.05	-11.43	-11.48 ± 0.05
	873.1	-0.054	-10.29	0.01	-10.06	-10.17 ± 0.01
	963.9	-0.054	-9.17	0.03	-9.00	-9.04 ± 0.03
	1053.3	-0.054	-8.22	0.05	-8.13	-8.10 ± 0.05
Tb	801.3	-0.092	-10.92	0.21	–	-10.70 ± 0.21
	899.9	-0.092	-9.80	0.16	–	-9.59 ± 0.16
	998.5	-0.092	-8.66	0.25	–	-8.45 ± 0.25
	1095.0	-0.092	-7.73	0.10	–	-7.52 ± 0.10
Dy	813.8	-0.164	-11.04	0.04	–	-10.66 ± 0.04
	915.3	-0.164	-9.99	0.08	–	-9.62 ± 0.08
	993.8	-0.164	-9.12	0.06	–	-8.75 ± 0.06
	1088.8	-0.164	-8.23	0.04	–	-7.85 ± 0.04

^a The errors are the standard deviations of the data points around the fitted lines.

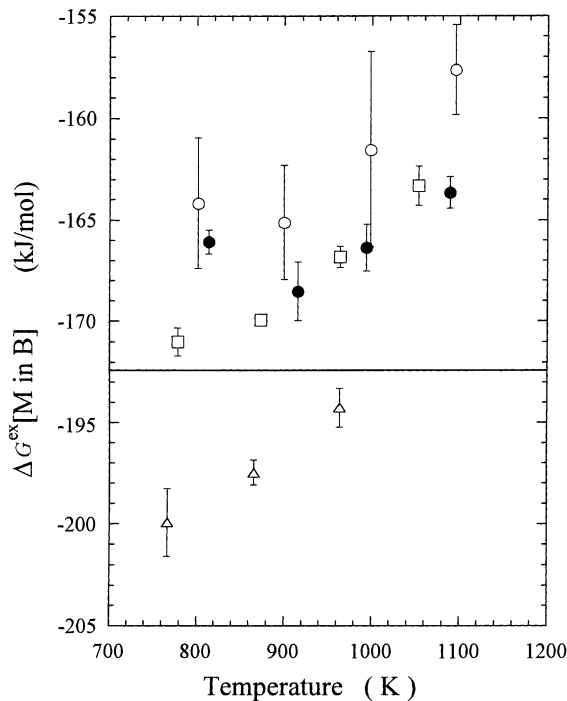


Fig. 3. Temperature dependence of excess Gibbs energy changes of La (Δ), Gd (\square), Tb (\circ) and Dy (\bullet), in liquid bismuth.

chemical form or structure of the dissolved species of M does not change in this temperature region. Thereby, for determining $\Delta H^{\text{ex}}[\text{M in B}]$ and $\Delta S^{\text{ex}}[\text{M in B}]$ by the temperature dependence of $\log f_{M(\text{in B})}$, a group of data

points showing a good linearity was selected for the analysis. Because, plotting $\log f_{M(\text{in B})}$ on $1/T$ provides more precise analysis for the determination of $\Delta H^{\text{ex}}[\text{M in B}]$ and $\Delta S^{\text{ex}}[\text{M in B}]$, $\log f_{M(\text{in B})}$'s sided to higher temperature were plotted in Fig. 4 and analyzed. The lines in the figures show the results of the least-squares fitting treatment, which gave quite satisfactory agreements to the data. By writing the linear functions as

$$\log f_{M(\text{in B})} = a1/T + b, \quad (8)$$

$\Delta H^{\text{ex}}[\text{M in B}]$ and $\Delta S^{\text{ex}}[\text{M in B}]$ are given by the following equations:

$$\Delta H^{\text{ex}}[\text{M in B}] \text{ (kJ/mol)} = 2.303Ra, \quad (9)$$

and

$$\Delta S^{\text{ex}}[\text{M in B}] \text{ (J/mol)} = -2.303Rb. \quad (10)$$

The determined *a* and *b* are given in Table 2, by which $\log f_{M(\text{in B})}$ can be calculated for any desired temperatures. Despite the concentration dependence of $\log f_{M(\text{in B})}$ which are given by Eq. (7) and the coefficients of Table 1, $\Delta H^{\text{ex}}[\text{M in B}]$ and $\Delta S^{\text{ex}}[\text{M in B}]$ are expected not to significantly depend on the concentration. This is responsible for the fact that the slopes of Eq. (7) are approximately common for all temperatures, as seen in Table 1, by which even different $\log x_{M(\text{in B})}$ give the same temperature dependence.

Table 3 summarizes the result of $\Delta H^{\text{ex}}[\text{M in B}]$ and $\Delta S^{\text{ex}}[\text{M in B}]$ in comparison with the literature values. The literature values of $\Delta H^{\text{ex}}[\text{M in B}]$ and $\Delta S^{\text{ex}}[\text{M in B}]$ were those calculated from the temperature dependence coefficients of $\log f_{M(\text{in B})}$ reported by Lebedev [4].

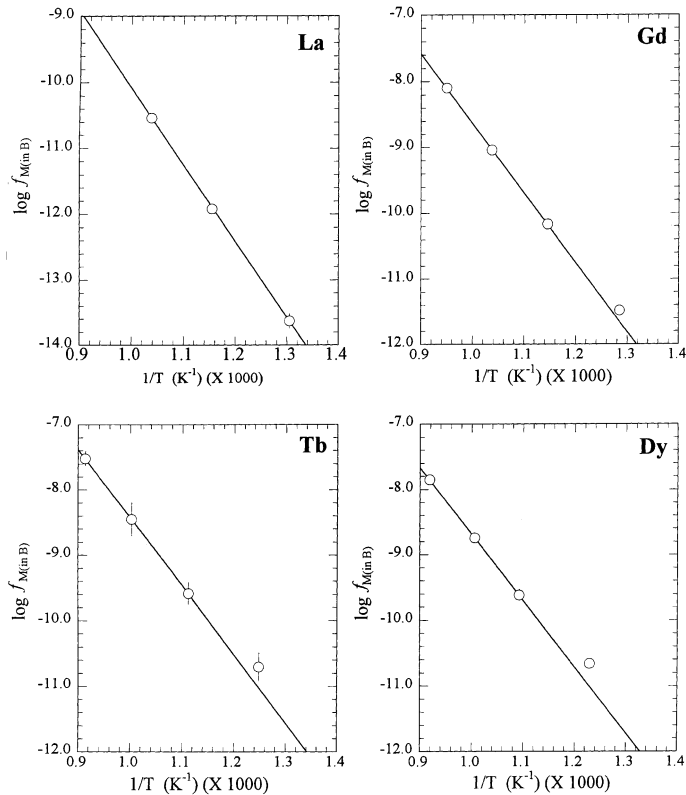


Fig. 4. Dependence of activity coefficients of La, Gd, Tb, and Dy on 1/T.

Table 2
Temperature dependence of $\log f_{M(\text{in B})}$ for $x_{M(\text{in B})} = 5 \times 10^{-3}$

	$\log f_{M(\text{in B})} = a/T + b$	
	<i>a</i>	<i>b</i>
La	-11572	1.47
Gd	-10564	1.92
Tb	-10438	2.01
Dy	-10123	1.44

$\Delta H^{\text{ex}}[M \text{ in B}]$ of La and Gd obtained in the present study agree with the literature values within the range of uncertainties.

4.3. Systematic variation of $\Delta H^{\text{ex}}[M \text{ in B}]$ along the lanthanide series

In the liquid alloy, it is presumably considered that the solute metal forms a chemical complex with the solvent metals, i.e., a cluster, and this is considered to be responsible for the thermodynamic excess stabilization of the solute metals [8]. Thus, the excess partial molar quantities of the solute metals in the solvent metals should reflect the degree of chemical bonding associated with the formation of the clusters. Generally, in the

chemistry of lanthanides, it is understood that the 4f-orbitals of lanthanides do not play a significant role in forming a bonding with the ligands. Thus, in most cases of the compounds of lanthanides, their chemical stabilities scarcely depend on the number of 4f-electrons, and hence they show a monotonic dependence only on their ionic radii [9]. Thus, the chemical stabilities of lanthanide compounds tend to show monotonic variations along the lanthanide series [9]. In contrast to this general understanding on the inorganic compounds of lanthanides, the thermodynamic stabilities of liquid alloy of lanthanides have not been sufficiently discussed from a similar viewpoint of the systematic variations along the lanthanide series. Determined $\Delta H^{\text{ex}}[M \text{ in B}]$ in this study, together with the reported values, provides a good opportunity for discussing the characteristic intermetallic interactions of lanthanide metals with bismuth.

From Miedema's semi-empirical model [10,11], the enthalpy change of solution of metal A into metal B which is denominated as $\Delta H_{\text{sol}}[A \text{ in B}]$ is given by

$$\Delta H_{\text{sol}}[A \text{ in B}] = V^{2/3} \frac{2P}{n_b(\text{A})^{-1/3} + n_b(\text{B})^{-1/3}} \times \left[-(\Delta\phi)^2 + \frac{Q}{P}(\Delta n_b^{1/3})^2 - \frac{R}{P} \right], \quad (11)$$

Table 3
 $\Delta H^{\text{ex}}[M \text{ in } B]$ and $\Delta S^{\text{ex}}[M \text{ in } B]$ determined and reported

	$V^{2/3}$ (cm ² /mol ^{2/3})	$\Delta H^{\text{ex}}[M \text{ in } B]$ (kJ/mol)		$\Delta S^{\text{ex}}[M \text{ in } B]$ (J/mol)	
		Lebedev et al. ^a	This study	Lebedev et al. ^a	This study
La	7.98	−219.15	−221.54 ± 2.31	−22.93	−28.11 ± 2.71
Ce	7.76	−225.77		−45.96	
Pr	7.56	−237.45		−63.31	
Nd	7.51	−220.07		−42.68	
Pm	7.43				
Sm	7.37				
Eu	7.36				
Gd	7.34	−200.89	−202.25 ± 1.80	−30.95	−36.84 ± 1.88
Tb	7.2		−199.83 ± 0.55		−38.49 ± 0.56
Dy	7.12		−193.80 ± 0.99		−27.69 ± 1.00
Ho	7.06				
Er	6.98	−182.46		−32.75	
Tm	6.9				
Yb	6.86				
Lu	6.81				

^a Derived from [4].

where V is the molar volume of metal A, $n_b(A)$ and $n_b(B)$ are the electron densities at the boundary of Wigner–Seitz cell, $\Delta\phi$ is the difference of electronegativities between A and B, and P, Q, R are the specific constants [10,11]. It should be remembered that R is an additional negative term necessary to account for the experimental results of transition-metals and polyvalent non-transition metals. Thus, R represents the degree of an additional metallic bonding that is not accounted for only by the difference of electronegativities and electron densities of A and B. R/P is recommended to be commonly 1.175 for the pair of any lanthanide and bismuth.

This number is obtained by multiplying a reduction factor of 0.73, a correction factor for the liquid alloy, to the number for the solid alloy [10,11].

By introducing a new factor F which encompasses all terms other than $V^{2/3}$, Eq. (11) yields

$$\Delta H_{\text{sol}}[A \text{ in } B] = V^{2/3} F(n_b(A), n_b(B), \Delta\phi, P, Q, R). \quad (12)$$

The parameters of lanthanides needed for Miedema's calculation, and the resulting F are listed in Table 4 [11]. In the previous study [3], we pointed out that, as long as

Table 4
 Parameters for Miedema's semi-empirical model^a

	$V^{2/3}$ [10] (cm ² /mol ^{2/3})	ϕ [10] (V)	$n_b^{1/3}$ [10] (du ^{1/3}) ^b	F (kJ/mol/cm ² mol ^{2/3})
La	7.98	3.17	1.18	−30.7
Ce	7.76	3.18	1.19	−30.5
Pr	7.56	3.19	1.20	−30.2
Nd	7.51	3.19	1.20	−30.2
Pm	7.43	3.19	1.21	−30.2
Sm	7.37	3.20	1.21	−29.9
Eu	7.36	3.20	1.21	−29.9
Gd	7.34	3.20	1.21	−29.9
Tb	7.20	3.21	1.22	−29.6
Dy	7.12	3.21	1.22	−29.6
Ho	7.06	3.22	1.22	−29.4
Er	6.98	3.22	1.23	−29.3
Tm	6.90	3.22	1.23	−29.3
Yb	6.86	3.22	1.23	−29.3
Lu	6.81	3.22	1.24	−29.2
Bi	7.20	4.15	1.16	

^a $P = 12.3$ (Ref. [10]); $Q/P = 0.944$ (Ref. [10]); $R/P = 1.175$ (Ref. [10]), $0.7(\text{Lanthanide}) \times 2.3(\text{bismuth}) \times 0.73(\text{reduction factor for liquid alloy})$.

^b $du = 6 \times 10^{22}$ electrons/cm³.

P, Q, R are common for all the lanthanides, F is approximately kept constant over the lanthanide series, and thus $\Delta H_{\text{sol}}[\text{M in B}]$ for lanthanides approximately should show a linear dependency on $V^{2/3}$.

Determined $\Delta H^{\text{ex}}[\text{M in B}]$ and reported values are plotted in Fig. 5 as functions of $V^{2/3}$. The lines drawn in Fig. 5 are those calculated by Eq. (11) with different values of R/P . The dotted line in Fig. 5 is obtained with $R/P = 1.175$, which was a value recommended by Alonso et al. [11]. This line clearly lies lower than the determined $\Delta H^{\text{ex}}[\text{A in B}]$ s, and thus this line should be understood as an estimate which is too negative. In Fig. 5, the line calculated with $R/P = 0.99$ appears to be rather suitable for the data points of La, Gd, Tb, Dy, and Er. On the other hand, the data points of Ce, Pr, and Nd locate much lower than this line, and this indicates that these elements may be singularly apart from the linear trend shown by La, Gd, Tb, Dy, and Er. Accordingly, $\Delta H^{\text{ex}}[\text{M in B}]$ of lanthanide appears to be divided into two groups; one which satisfies Miedema's semi-empirical rule with the use of $R/P = 0.99$ (La, Gd, Tb, Dy, and Er), and another which shows additionally

negative values than the first group (Ce, Pr, and Nd). For the first group, R/P is constantly 0.99. It is suggested that elements of the first group are controlled by the metallic volume, electron density, and electronegativity difference, and hence they show a monotonic variation. On the contrary, those belonging to the second group are likely to gain additional stabilization than the first group. Since the good agreement of determined values of La and Gd with the literature values convinces us to believe that the measurements of the first group are quite reliable, the linear relation of the first group with $R/P = 0.99$ is likely to validate the adaptation of Miedema's rule to the lanthanide series. Although there is a further need of re-measurements for Ce, Pr, and Nd to confirm their singularities, it should be noted that the second group has differently featured phase diagrams from those of the first group. From the reported phase diagrams of binary alloys of the second group elements [12], i.e., Ce, Pr, and Nd, an intermetallic compound MBi_2 is formed. In contrast, none of the first group elements, i.e., La, Gd, Tb, Dy, and Er, forms MBi_2 , and thus MBi is the intermetallic compound of the highest bismuth content. It is likely that this difference of the compound formation of the second group is incorporated into their thermodynamic stabilization in the liquid phase, and thus indicates different systematics from the first group. Further experimental measurements for the second group elements and other untested elements are strongly desired.

The systematic trend of $\Delta S^{\text{ex}}[\text{M in B}]$ along the lanthanide series cannot be obviously found in the values listed in Table 3, but, it would appear that $\Delta S^{\text{ex}}[\text{M in B}]$ of the second group elements are slightly more negative than the first group. This may also be linked to the singularity in $\Delta H^{\text{ex}}[\text{M in B}]$, and this possibly suggests the structural difference of the clusters in the liquid metal.

5. Conclusions

By adapting an EMF measurement to La, Gd, Tb, and Dy, their $\Delta G^{\text{ex}}[\text{M in B}]$ and $\log f_{\text{M(in B)}}$ in liquid bismuth were determined, and their dependences on the temperature and concentrations were analyzed. Through the temperature dependence of $\log f_{\text{M(in B)}}$, $\Delta H^{\text{ex}}[\text{M in B}]$ and $\Delta S^{\text{ex}}[\text{M in B}]$ were determined, and the systematic variation of $\Delta H^{\text{ex}}[\text{M in B}]$ along the lanthanide series was discussed. It was found that $\Delta H^{\text{ex}}[\text{M in B}]$'s of La, Gd, Tb, Dy, and Er satisfy Miedema's semi-empirical rule for mixing two liquid metals with the use of newly determined constant $R/P = 0.99$. Ce, Pr, and Nd were found to deviate from this rule, and their uniqueness was discussed in conjunction with the characteristics of their intermetallic compound.

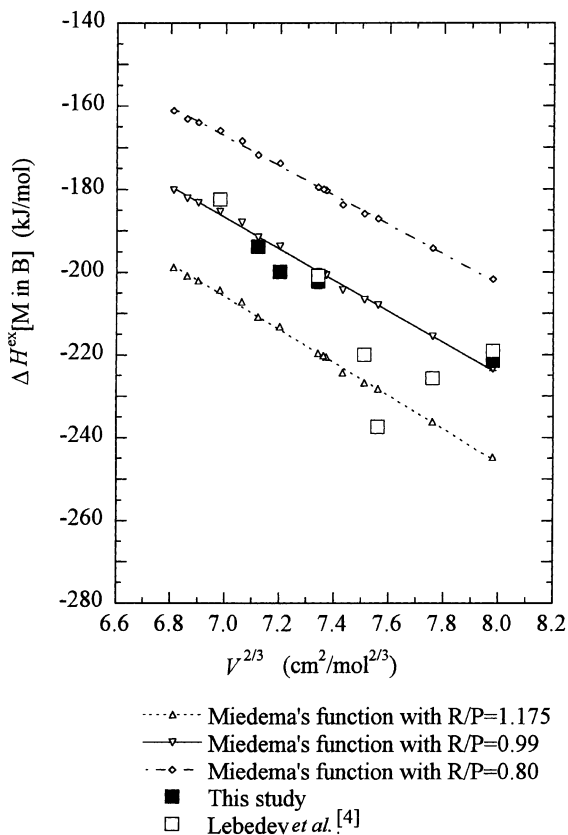


Fig. 5. Excess enthalpy changes of lanthanides in liquid bismuth as a function of $V^{2/3}$.

Acknowledgements

Authors are indebted to Dr Masaki Kurata of Central Research Institute of Electric Power Industry for his valuable advise about the experimental techniques. Authors are indebted to Dr Keizo Kawamoto, Mr Sataro Nishikawa, Dr Jitsuya Takada, Mr Hisao Kodaka and Mr Kiyomi Miyata of the Research Reactor Institute, Kyoto University for their technical support in the experimental activities. Authors wish to thank Mr Roy Jacobus for his help in the checking of the English expressions of this article.

References

- [1] H. Moriyama, H. Yamana, S. Nishikawa, Y. Miyashita, K. Moritani, T. Mitsugashira, *J. Nucl. Mater.* 247 (1997) 197.
- [2] H. Moriyama, H. Yamana, S. Nishikawa, S. Shibata, N. Wakayama, Y. Miyashita, K. Moritani, T. Mitsugashira, *J. Alloys Compounds* 271–273 (1998) 587.
- [3] H. Yamana, N. Wakayama, N. Souda, H. Moriyama, *J. Nucl. Mater.* 278 (2000) 37.
- [4] V.A. Lebedev, *Selectivity of Liquid Metal Electrodes in Molten Halides*, Metallurgiya, Chelyabinsk, 1993 (in Russian).
- [5] V.I. Kober, V.A. Lebedev, I.F. Nichkov, S.P. Raspopin, *Russ. J. Phys. Chem.* 42 (4) (1968) 360.
- [6] V.I. Kober, V.A. Lebedev, I.F. Nichkov, S.P. Raspopin, *Russ. J. Phys. Chem.* 45 (4) (1971) 313.
- [7] O. Knacke, O. Kubaschewski, K. Hesselmann (Eds.), *Thermochemical Properties of Inorganic Substances*, 2nd Ed., Springer, Berlin, 1991.
- [8] R.N. Singh, N.H. March, *Intermetallic Compounds – Principle and Practice*, Wiley, Baffins, 1995, ch. 28.
- [9] L.R. Morss, in: K.A. Gschneidner Jr., L. Eyring, G.R. Choppin, G.H. Lander (Eds.), *Handbook of the Physics and Chemistry of Rare Earths*, vol. 18, North-Holland, Amsterdam, 1994, ch. 122.
- [10] F.R. DeBoer, R. Boom, W.C. Mattens, A.R. Miedema, A.K. Niessen, *Cohesion in Metals-Transition Metal Alloys*, North-Holland, Amsterdam, 1988.
- [11] J.A. Alonso, N.H. March, *Electrons in Metals and Alloys*, Academic Press, London, 1989.
- [12] B.M. Thaddeus, H. Okamoto, P.R. Subramanian, L. Kacprzak (Eds.), *Binary Alloy Phase Diagrams*, 2nd Ed., ASM International, Metals Park, OH, 1990.